

Lung Abnormalities Detected with Hyperpolarized ^{129}Xe MRI in Patients with Long COVID


James T. Grist, BSc, PhD • Guilhem J. Collier, PhD • Huw Walters, MBBS • Minsuok Kim, PhD • Mitchell Chen, BMBCb, MEng, DPhil, FRCR • Gabriele Abu Eid, BSc • Aviana Laws • Violet Matthews, BSc • Kenneth Jacob, BSc • Susan Cross, BSc • Alexandra Eves, BSc • Marianne Durrant, BSc • Anthony McIntyre, BAppSci • Roger Thompson, PhD • Rolf F. Schulte, PhD • Betty Raman, MBBS, DPhil • Peter A. Robbins, PhD • Jim M. Wild, PhD, MSc, MA • Emily Fraser, PhD, MBCbB, BSc • Fergus Gleeson, MBBS

From the Department of Radiology (J.T.G., H.W., M.C., G.A.E., A.L., V.M., K.J., S.C., A.E., M.D., A.M., F.G.) and Oxford Interstitial Lung Disease Service (E.F.), Oxford University Hospitals NHS Trust, Oxford, UK; Department of Physiology, Anatomy, and Genetics (J.T.G., P.A.R.), Radcliffe Department of Medicine, Oxford Centre for Clinical Magnetic Resonance Research (J.T.G., B.R.), and Department of Oncology (F.G.), University of Oxford, Old Road Headington, Oxford OX3 7DQ, UK; Institute of Cancer and Genomic Sciences, University of Birmingham, Birmingham, UK (J.T.G.); POLARIS, Department of Infection Immunity and Cardiovascular Disease (G.J.C., J.M.W.), and Department of Infection, Immunity, and Cardiovascular Disease (R.T.), University of Sheffield, Sheffield, UK; Wolfson School of Mechanical, Electrical and Manufacturing Engineering, Loughborough University, Loughborough, UK (M.K.); and GE Healthcare, Munich, Germany (R.F.S.). Received January 12, 2022; revision requested February 23; revision received April 25; accepted May 13. **Address correspondence to** F.G. (email: fgleeson@mac.com).

Supported by the University of Oxford, the NIHR Oxford Biomedical Research Centre, the National Consortium of Intelligent Medical Imaging, the National Institutes of Health Research, and the British Heart Foundation Oxford Centre of Research Excellence. The Sheffield collaborators are also supported by the Medical Research Council (MRC/MR/M008894/1).

Conflicts of interest are listed at the end of this article.

See also the editorial by Parraga and Matheson in this issue.

Radiology 2022; 305:709–717 • <https://doi.org/10.1148/radiol.220069> • Content codes: 

Background: Post-COVID-19 condition encompasses symptoms following COVID-19 infection that linger at least 4 weeks after the end of active infection. Symptoms are wide ranging, but breathlessness is common.

Purpose: To determine if the previously described lung abnormalities seen on hyperpolarized (HP) pulmonary xenon ^{129}Xe MRI scans in participants with post-COVID-19 condition who were hospitalized are also present in participants with post-COVID-19 condition who were not hospitalized.

Materials and Methods: In this prospective study, nonhospitalized participants with post-COVID-19 condition (NHLC) and posthospitalized participants with post-COVID-19 condition (PHC) were enrolled from June 2020 to August 2021. Participants underwent chest CT, HP ^{129}Xe MRI, pulmonary function testing, and the 1-minute sit-to-stand test and completed breathlessness questionnaires. Control subjects underwent HP ^{129}Xe MRI only. CT scans were analyzed for post-COVID-19 interstitial lung disease severity using a previously published scoring system and full-scale airway network (FAN) modeling. Analysis used group and pairwise comparisons between participants and control subjects and correlations between participant clinical and imaging data.

Results: A total of 11 NHLC participants (four men, seven women; mean age, 44 years \pm 11 [SD]; 95% CI: 37, 50) and 12 PHC participants (10 men, two women; mean age, 58 years \pm 10; 95% CI: 52, 64) were included, with a significant difference in age between groups ($P = .05$). Mean time from infection was 287 days \pm 79 (95% CI: 240, 334) and 143 days \pm 72 (95% CI: 105, 190) in NHLC and PHC participants, respectively. NHLC and PHC participants had normal or near normal CT scans (mean, 0.3/25 \pm 0.6 [95% CI: 0, 0.63] and 7/25 \pm 5 [95% CI: 4, 10], respectively). Gas transfer (DLCO) was different between NHLC and PHC participants (mean DLCO, 76% \pm 8 [95% CI: 73, 83] vs 86% \pm 8 [95% CI: 80, 91], respectively; $P = .04$), but there was no evidence of other differences in lung function. Mean red blood cell-to-tissue plasma ratio was different between volunteers (mean, 0.45 \pm 0.07; 95% CI: 0.43, 0.47) and PHC participants (mean, 0.31 \pm 0.10; 95% CI: 0.24, 0.37; $P = .02$) and between volunteers and NHLC participants (mean, 0.37 \pm 0.10; 95% CI: 0.31, 0.44; $P = .03$) but not between NHLC and PHC participants ($P = .26$). FAN results did not correlate with DLCO) or HP ^{129}Xe MRI results.

Conclusion: Nonhospitalized participants with post-COVID-19 condition (NHLC) and posthospitalized participants with post-COVID-19 condition (PHC) showed hyperpolarized pulmonary xenon ^{129}Xe MRI and red blood cell-to-tissue plasma abnormalities, with NHLC participants demonstrating lower gas transfer than PHC participants despite having normal CT findings.

© RSNA, 2022

Online supplemental material is available for this article.

On March 11, 2020, COVID-19 was declared a global pandemic by the World Health Organization. Beyond the acute respiratory manifestations of COVID-19 infection, which can result in severe illness, hospitalization, and death, the medium- and long-term problems experienced by people after COVID-19 can be considerable (1). Large-cohort studies have revealed that symptoms can persist for months after the initial infection in participants hospitalized with COVID-19 pneumonia and in those whose

disease was managed in the community. The presence of ongoing symptoms related to prior COVID-19 infection has been defined by the World Health Organization as the post-COVID-19 condition. Although over 200 symptoms have been reported, the most common problems are those of breathlessness, fatigue, and brain fog (2). Post-COVID-19 condition presents a global health burden, with many people unable to return to normal activities or employment months after they first became unwell.

This copy is for personal use only. To order printed copies, contact reprints@rsna.org

Abbreviations

DLCO = total lung diffusion capacity for carbon monoxide, FAN = full-scale airway network, HP = hyperpolarized, mBORG = modified Borg score, NHLC = nonhospitalized participant with post-COVID-19 condition, PHC = posthospitalized participant with post-COVID-19 condition, RBC:TP = red blood cell to tissue plasma

Summary

Hyperpolarized xenon 129 MRI and total lung diffusion capacity for carbon monoxide demonstrate significantly impaired gas transfer in nonhospitalized participants with post-COVID-19 condition and normal chest CT findings.

Key Results

- In a prospective study of 11 participants, there were significant differences in mean red blood cell–to–tissue plasma ratio between healthy volunteers and posthospitalized participants with post-COVID-19 condition (PHC) and nonhospitalized participants with post-COVID-19 condition (NHLC), indicating potential differences in lung function.
- NHLC participants had near normal CT scores, and diffusing capacity of lung for carbon monoxide in NHLC and PHC participants was significantly lower than that in healthy volunteers, potentially indicating a decrease in lung function but not structure.

Chest radiography is the most common imaging modality for the diagnostic work-up of acute COVID-19 pneumonia, and it is often repeated 3 months after the acute infection in patients who required hospital admission. Chest CT may be performed to investigate persistent breathlessness if the chest radiography findings are normal or if there are other concerns regarding COVID-19–related lung damage. In a small proportion of participants, interstitial lung abnormalities persist, and evidence of post-COVID fibrosis has been reported (3,4). These abnormalities may account for dyspnea, but in most individuals with post-COVID-19 condition, CT findings are normal or nearly normal. Similarly, lung function tests usually reveal values within the normal range. A recent study looking at a small cohort of posthospitalized participants with post-COVID-19 condition (PHC) at 3 months after hospital discharge reported that hyperpolarized (HP) xenon 129 (^{129}Xe) MRI enabled detection of alveolar gas transfer abnormalities even when the CT scans and lung function test results were normal or nearly normal (5). HP ^{129}Xe MRI enables assessment of ventilation and gas transfer across the alveolar epithelium into red blood cells. It provides regional information on pulmonary vasculature integrity and may enable identification of lung abnormalities not apparent on CT scans (6).

In individuals with post-COVID-19 condition, a breathing pattern disorder is commonly identified and contributes to breathlessness in a substantial proportion of these individuals (7); however, whether there are additional reasons for this breathlessness remains unclear. The purpose of this study was to determine whether the previously described lung abnormalities seen on HP ^{129}Xe MRI scans in the PHC group are also present in nonhospitalized participants with post-COVID-19 condition (NHLC) (5).

Materials and Methods

Participant Recruitment and Screening

This prospective study was approved by the Healthy Research Authority (research ethics committee reference 20/NW/0235), and all participants gave written informed consent. Consecutive participants were recruited from the Oxford Post-COVID Assessment Clinic, with the following inclusion criteria: In the PHC group, participants had reverse transcription–polymerase chain reaction proof of SARS-CoV-2 infection and no history of intubation, more than 3 months had passed since discharge, there was no prior history of interstitial lung or airways disease, nor was there a smoking history of more than 10 pack-years, and CT findings were normal or nearly normal. In the NHLC group, participants had reverse transcription–polymerase chain reaction or positive antibody proof of SARS-CoV-2 infection, they were not hospitalized during acute infection, there was no evidence of interstitial lung or airways disease, nor was there a smoking history of more than 10 pack-years, and CT findings were normal or nearly normal.

For both cohorts, diagnosis of post-COVID-19 condition was made after referral to a specialist clinic with medically unexplained dyspnea as a symptom and in accordance with National Institute for Health and Care Excellence diagnostic criteria.

Healthy volunteers were recruited from the local staff pool at the University of Sheffield and the University of Oxford. Volunteers had to have no previous evidence of COVID-19 infection with reverse transcription–polymerase chain reaction testing and no clinically relevant history of lung or cardiovascular disease or smoking history. We did allow a volunteer with mild well-controlled asthma and no evidence of airway obstruction at spirometry to be included (Fig 1).

Imaging Protocol and Physiologic Measurements

Imaging was performed at 1.5 T (HDx; GE Healthcare) with a dedicated xenon transmit–receive coil (CMRS), and proton im-

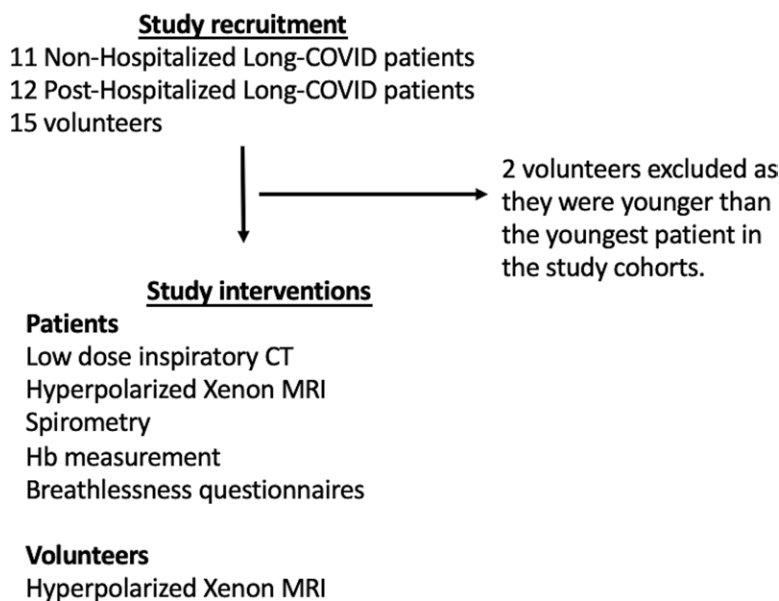


Figure 1: Study flowchart. Hb = hemoglobin.

ages were acquired with the body coil. When possible, participants underwent HP ^{129}Xe MRI scanning twice, with the second scan being performed approximately 1 hour after the first.

A three-dimensional four-echo flyback radial acquisition was used to acquire dissolved-phase HP ^{129}Xe MRI scans, as previously described (8). Sequence parameters were as follows: repetition time per spoke, 23 msec; one breath hold; acquired and reconstructed image resolution of 1.75 and 0.875 cm, respectively, in all dimensions; nominal flip angle per excitation on dissolved and gas phases, 40° and 0.7° , respectively; and total scanning time, 16 seconds. Gas, tissue plasma, and red blood cell images were reconstructed.

The noise level for each image was calculated on a section-by-section basis. Any voxels in the tissue plasma mask in each section that were less than five times the median noise level in the section were discarded. Ratiometric maps (red blood cell-to-tissue plasma [RBC:TP] ratio) were then calculated on a voxel-by-voxel basis. The mean \pm SD and coefficient of variation for each ratiometric map were then calculated on a participant-by-participant basis.

All trial participants underwent contemporaneous low-dose CT (General Electric) after inspiration of 1 L of room air, with a section thickness of 0.625 mm. Images were reviewed by a radiologist (H.W.) with 5 years of experience who was blinded to clinical data and ^{129}Xe MRI results, as previously described (5). A subset of participants' CT data (nine NHL participants, five PHC participants) underwent full-scale airway network (FAN) modeling analysis using the previously reported technique (9).

They also underwent spirometry; measurement of hemoglobin level, gas transfer, and Dyspnea-12 score; as well as a 1-minute sit-to-stand test. The number of repetitions was recorded alongside the modified Borg (mBORG) score and oxygen saturations before and after a 1-minute sit-to-stand test.

Statistical Analyses

Initial analysis was performed for each cohort independently, with correlation between clinical and imaging variables assessed using Spearman correlation and with a subsequent linear fit performed for significantly correlated variables. Correlations between D_{LCO} , mean RBC:TP value, and FAN analysis parameters were performed using Spearman correlation. The Mann-Whitney U test was used to assess for differences in FAN parameters between NHL and PHC cohorts.

Participant data were separated into NHL and PHC groups, and the previously mentioned analyses were reperformed for group-dependent associations with clinical symptoms.

Comparisons between RBC:TP ratio in participant and volunteer groups were assessed using nonparametric analysis of variance and Tukey post hoc tests with Bonferroni correction for multiple comparisons. When data were available only for participants (eg, for mBORG and lung function data), a two-sided t test was used to compare cohorts. The intraclass correlation coefficient was calculated to assess repeatability of mean RBC:TP ratio using data from the repeated HP ^{129}Xe MRI scans. $P < .05$ was assumed to indicate a significant difference. All analyses were performed using statistical software (The R Project; The R

Foundation). Unless otherwise stated, all data are presented as mean \pm SD, with 95% CI included.

Results

Participant Characteristics

A total of 11 NHL (seven women) and 12 PHC (two women) participants were recruited, with mean ages of 44 years \pm 1 (95% CI: 37, 50) and 58 years \pm 10 (95% CI: 52, 64) ($P = .05$), respectively (Tables 1, 2). CT, proton, and fused RBC:TP and proton images from NHL and PHC participants are shown in Figures 2 and 3, respectively. Thirteen healthy volunteers (mean age, 41 years \pm 11; 95% CI: 30, 52; six women) were recruited and underwent HP ^{129}Xe MRI. Example proton and fused RBC:TP and proton images obtained in a volunteer are shown in Figure E1 (online). The mean time from infection in the NHL and PHC participants was 287 days \pm 79 (95% CI: 240, 334) and 149 days \pm 68 (95% CI: 105, 190) ($P < .01$), respectively.

Mean hemoglobin levels for NHL and HLC participants were 144 g/L \pm 15 (95% CI: 134, 153) and 145 g/L \pm 14 (95% CI: 133, 150), respectively. NHL and PHC participants exhibited breathlessness, with mean Dyspnea-12 scores of 9 \pm 5 (95% CI: 6, 12) and 10 \pm 5 (95% CI: 7, 12) ($P = .67$), respectively; mBORG before and after the sit-to-stand test was 2 \pm 2 (95% CI: 0.8, 3) and 7 \pm 1 (95% CI: 6, 7), respectively, in NHL participants and 2 \pm 2 (95% CI: 0.5, 3) and 5 \pm 1 (95% CI: 4, 6), respectively, in PHC participants ($P < .05$ in all cases). There was no evidence of differences in oxygen saturations before and after mBORG sit-to-stand test (mean, 97.06% \pm 0.02 [95% CI: 96, 98] vs 97.59% \pm 0.02 [95% CI: 97, 99] oxygen saturation before vs after; $P = .99$). The majority of NHL and PHC participants (nine of 11 and four of five, respectively) were in the bottom 2.5th percentile for the number of repetitions they could do for the mBORG sit-to-stand test (range, 2.5–75 repetitions and 2.5–25 repetitions, respectively) (10). There was no significant difference between NHL and PHC participants for CT score (0.3 \pm 0.6 [95% CI: 0, 0.6] and 7 \pm 5 [95% CI: 4, 11], respectively; $P < .01$).

Lung Function and Imaging Results

The mean RBC:TP value and coefficient of variation for NHL participants, PHC participants, and healthy volunteers are shown in Figure 4. There were significant differences in mean RBC:TP value between volunteers (0.46 \pm 0.07; 95% CI: 0.43, 0.47) and PHC participants (0.31 \pm 0.10; 95% CI: 0.24, 0.37) and between volunteers and NHL participants (0.37 \pm 0.10; 95% CI: 0.31, 0.44) (adjusted $P < .05$ in all cases); however, there were not significant differences between PHC and NHL participants ($P = .29$). Of note, seven of 11 NHL participants and 11 of 12 PHC participants had an RBC:TP value that was more than 2 SDs of the mean from mean RBC:TP value in healthy volunteers.

There was no significant difference between NHL participants and PHC participants in mean percentage forced expiratory volume or forced vital capacity (100% \pm 13 [95% CI: 92,

Table 1: Data for Each Nonhospitalized Participant with Post-COVID-19 Condition

Patient No.	Age at Examination (y)	Sex	Hb Level (g/L)	Time from Infection (d)	FEV (%)	TLco (%)	CT Score	RBC:TP*	RBC:TP			mBORG Pre	mBORG Post	No. of Respirations in 1 Minute	Percentile for Age and Sex
									Coeff Var	Dysp-12					
1	61	M	141	210	104	80	0	0.31 ± 0.31	0.34	NA	0	7	21	2.5	
2	39	M	161	393	106	NA	0	0.49 ± 0.14	0.28	5	0	5	58	75	
3	39	F	125	437	102	77	0	0.32 ± 0.13	0.40	10	1	8	30	2.5	
4	51	F	NA	394	123	NA	0	0.42 ± 0.13	0.31	11	2	8	30	2.5	
5	28	M	166	263	72	83	0	0.51 ± 0.13	0.27	0	0	5	18	2.5	
6	46	F	122	213	98	73	0	0.24 ± 0.11	0.47	7	5	8	21	2.5	
7	59	F	142	260	105	89	2	0.29 ± 0.12	0.40	16	3	7	27	2.5	
8	55	F	145	261	97	65	0	0.33 ± 0.09	0.27	7	3	8	22	2.5	
9	34	F	143	294	101	83	1	0.41 ± 0.12	0.28	12	3	7	61	75	
10	38	F	128	246	83	66	0	0.26 ± 0.06	0.23	21	3	6	21	2.5	
11	29	M	166	166	111	87	0	0.58 ± 0.17	0.29	5	0	4	29	2.5	

Note.—Coeff Var = coefficient of variation, FEV = forced expiratory volume, Hb = hemoglobin, mBORG = modified Borg score, NA = not acquired, RBC:TP = red blood cell-to-tissue or plasma ratio, TLco = transfer capacity of the lung for carbon monoxide.

* Data are mean ± standard deviation.

Table 2: Data for Each Posthospitalized Participant with Post-COVID-19 Condition

Patient No.	Age at Examination (y)	Sex	Hb Level (g/L)	Time from Infection (d)	FEV (%)	TLco (%)	CT Score	RBC:TP*	RBC:TP			mBORG Pre	mBORG Post	No. of Respirations in 1 Minute	Percentile for Age and Sex
									Coeff Var	Dysp-12					
1	62	M	156	129	92	NA	10	0.37 ± 0.13	0.36	NA	NA	NA	NA	NA	NA
2	69	M	160	169	114	NA	5	0.31 ± 0.08	0.28	NA	NA	NA	NA	NA	NA
3	56	F	122	195	108	100	3	0.32 ± 0.10	0.31	14	NA	NA	NA	NA	NA
4	66	M	146	192	109	89	2	0.29 ± 0.11	0.39	NA	NA	NA	NA	NA	NA
5	62	M	130	68	76	71	7	0.22 ± 0.11	0.47	15	NA	NA	NA	NA	NA
6	69	M	137	212	119	95	15	0.25 ± 0.08	0.34	11	1	2	21	2.5	
7	55	F	131	269	69	79	23	0.28 ± 0.11	0.39	5	1	5	23	2.5	
8	55	M	133	26	62	85	14	0.16 ± 0.08	0.50	1	1	5	31	2.5	
9	29	M	142	84	95	NA	0	0.59 ± 0.15	0.25	NA	NA	NA	NA	NA	NA
10	62	M	165	101	54	90	7	0.33 ± 0.15	0.46	NA	5	8	25	2.5	
11	60	M	167	173	83	NA	12	0.34 ± 0.12	0.36	NA	0	6	31	25	2.5
12	48	M	147	159	76	77	14	0.28 ± 0.09	0.31	11	NA	NA	NA	NA	NA

Note.—Coeff Var = coefficient of variation, FEV = forced expiratory volume, Hb = hemoglobin, mBORG = modified Borg score, NA = not acquired, RBC:TP = red blood cell-to-tissue or plasma ratio, TLco = transfer capacity of the lung for carbon monoxide.

* Data are mean ± standard deviation.

108] and $88\% \pm 21$ [95% CI: 72, 97], respectively; $P < .05$), but there was a significant difference in mean D_{LCO} ($78\% \pm 8$ [95% CI: 73, 84] vs $86\% \pm 9$ [95% CI: 80, 91], respectively; $P = .04$).

In NHLc participants, there was a significant correlation between D_{LCO} and RBC:TP SD (correlation coefficient = 0.78, $P = .02$) and between RBC:TP mean and SD (correlation coefficient = 0.63, $P = .05$). Further correlations between RBC:TP and Dyspnea-12 score and between RBC:TP and mBORG after the 1-minute sit-to-stand test were almost significant ($P = .06$ and $P = .08$, respectively). Correlations between mean RBC:TP and SD are shown in Figure E2A (online), and correlations between D_{LCO} and RBC:TP SD are shown in Figure 5A.

In the PHC participants, there were significant correlations between participant age and the dissolved phase mean (correlation coefficient = -0.82 , $P < .01$; Fig E2B [online]), CT score, and RBC:TP SD (correlation coefficient = 0.54, $P = .04$; Fig 5B), RBC:TP mean and SD (correlation coefficient = 0.76, $P = .03$; Fig E2C [online]), and RBC:TP mean and coefficient of variation (correlation coefficient = -0.73 , $P = .04$; Fig E2D [online]). Ten PHC participants underwent repeat HP ^{129}Xe MRI, and the intra-class correlation coefficient of mean RBC:TP was 0.96 (95% CI: 0.87, 0.99) (lower-upper bound), indicating excellent repeatability (Table E1 [online]) (11). There were no significant correlations between D_{LCO} , mean RBC:TP, or any of the FAN parameters.

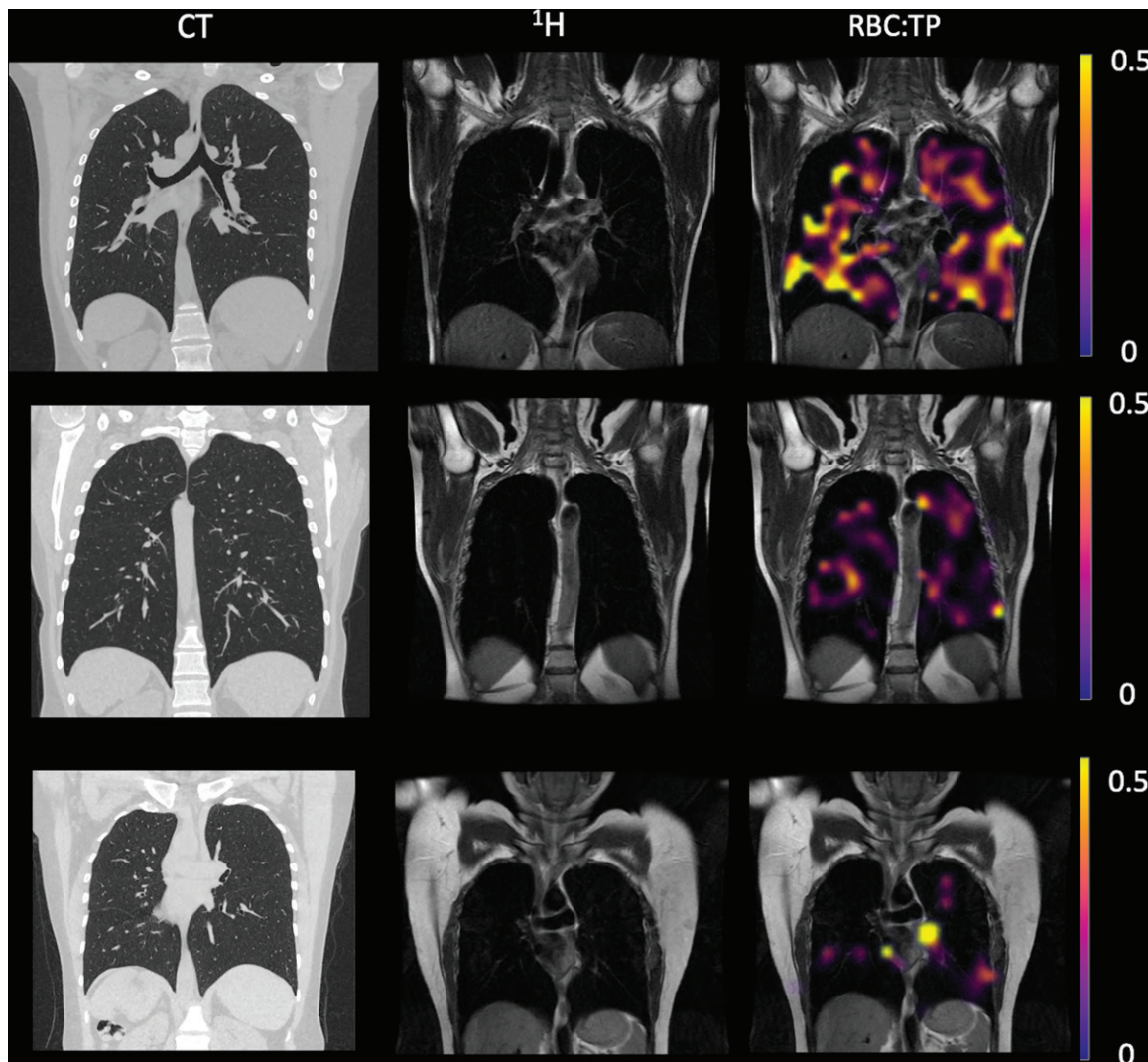


Figure 2: Example CT, proton (^1H), and proton and red blood cell-to-tissue plasma (RBC:TP) images in participants with post-COVID-19 condition. Top row: Images in a participant with an RBC:TP value of 0.49. Middle row: Images in a participant with an RBC:TP value of 0.31. Bottom row: Images in a participant with an RBC:TP value of 0.24. Imaging revealed little to no discernible damage on CT scans, yet highly heterogeneous and low RBC:TP values in the lungs of nonhospitalized participants with post-COVID-19 condition.

There was also no evidence of differences between FAN parameters in the nine NHLc participants and five PHc participants (all $P > .1$). FAN modeling results are shown in Figure 6.

Discussion

This pilot study used hyperpolarized (HP) xenon ^{129}Xe MRI to evaluate the lungs of nonhospitalized participants with post-COVID-19 condition (hereafter, NHLc participants) with unexplained breathlessness after clinical evaluation in a dedicated post-COVID clinic. We found that the NHLc participants had normal CT scans, and the posthospitalized participants with post-COVID-19 (hereafter, PHc participants) had normal or nearly normal CT scans ($0.3/25 \pm 0.6$ [95% CI: 0, 0.6] and $7/25 \pm 5$ [95% CI: 4, 11], respectively). Gas transfer (D_{LCO}) was significantly different between NHLc participants and PHc participants (mean, $76\% \pm 8$ [95% CI: 73, 84] vs $86\% \pm 8$ [95% CI: 80, 91], respectively; $P = .04$), but there was no evidence of other

differences in lung function. Mean red blood cell-to-tissue plasma (RBC:TP) value was significantly different between volunteers (0.45 ± 0.07 ; 95% CI: 0.43, 0.47) and PHc participants (0.31 ± 0.10 ; 95% CI: 0.24, 0.37; $P = .02$) and between volunteers and NHLc participants (0.37 ± 0.10 ; 95% CI: 0.31, 0.44; $P = .03$) but not between NHLc participants and PHc participants ($P = .26$).

All the NHLc participants in this study with abnormal HP ^{129}Xe MRI findings were imaged more than 6 months after their initial infection, indicating that these abnormalities were not a transient phenomenon after acute infection. The NHLc participants were also, on average, further from their initial infection than were the PHc participants (287 vs 149 days). Interestingly, the measured abnormality on HP ^{129}Xe MRI scans appears to be only marginally greater in the PHc participants than in the NHLc participants, despite participants who were admitted to the hospital having had a presumed clinically more severe acute infection.

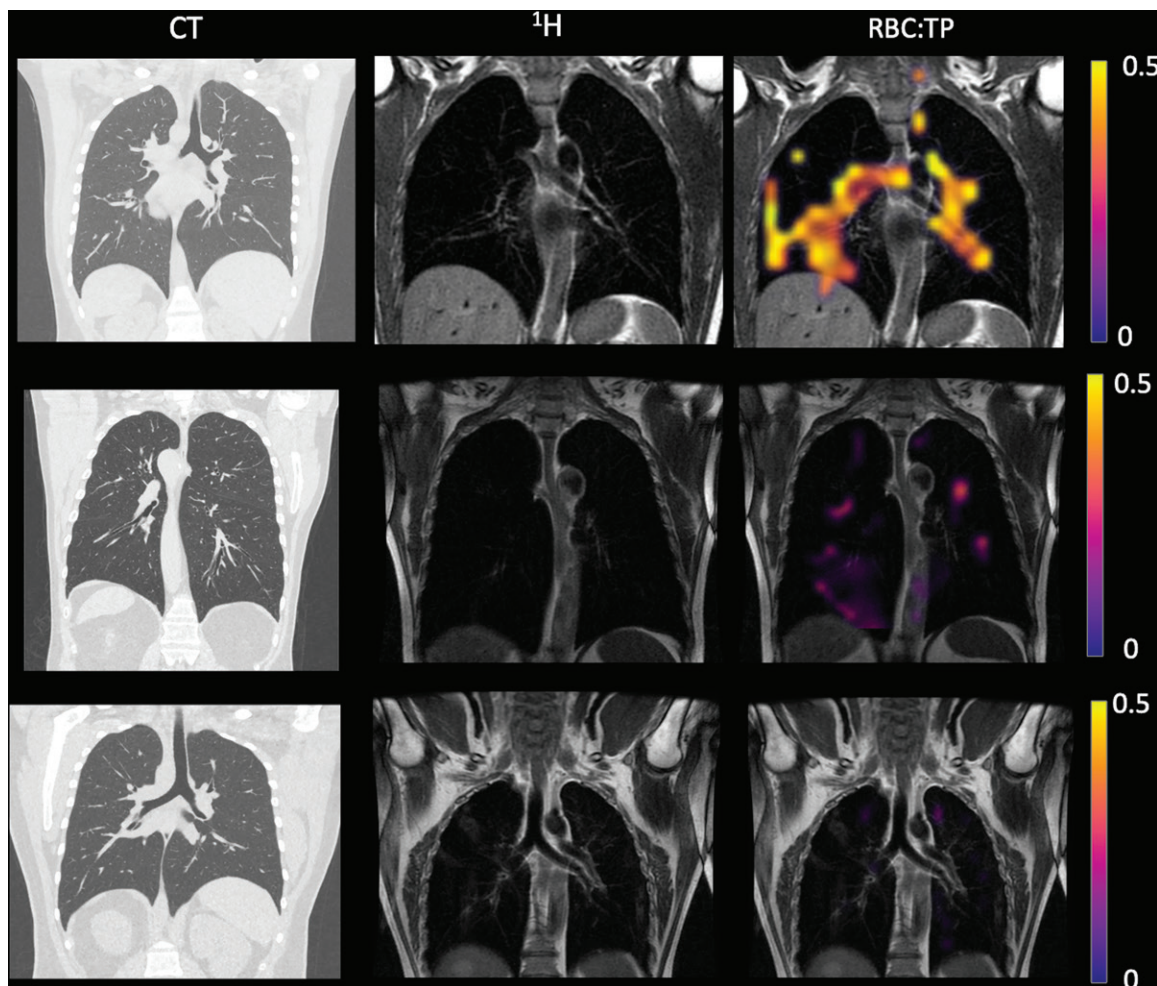


Figure 3: Example CT, proton (^1H), and proton and red blood cell-to-tissue plasma (RBC:TP) images in posthospitalized participants with post-COVID-19 condition. Top row: Images in a participant with an RBC:TP value of 0.59. Middle row: Images in a participant with an RBC:TP value of 0.31. Bottom row: Images in a participant with an RBC:TP value of 0.16. Imaging revealed minimal damage on CT scans, yet highly heterogeneous and low RBC:TP values in the lungs of posthospitalized participants.

The participants in this study were well matched according to phenotype, with symptoms typical of NHLC participants who did not require hospital admission (12). The relationship of the HP ^{129}Xe MRI abnormalities detected and the breathlessness experienced by the wider population of PHC participants whose disease was managed both in the hospital and in the community during their acute infection is unclear. Additionally, the pathophysiologic mechanisms that underlie the changes in HP ^{129}Xe MRI after COVID-19 infection have yet to be fully elucidated; however, it is possible to make some inferences regarding the nature of the underlying defect based on our results. It is known that inert gases (those that do not chemically react with blood) equilibrate rapidly in the lung (13), with xenon quickly reaching the red blood cells (14). RBC:TP is a composite of the ratio of two tissue volumes (the pulmonary capillary [plus potentially some pulmonary venous] blood volume to the alveolar membrane volume), gas transfer, and pulmonary blood flow measured using HP ^{129}Xe MRI. A lower number suggests that infection with Sars-CoV-2 may have induced some microstructural abnormality to one or two volumes, causing a reduction in blood volume, for example due

to widespread microclots (15), changes in pulmonary blood flow, a thickening of the alveolar membrane, or a combination thereof; any of these would be expected to cause a reduction in diffusing capacity (16).

It is possible that in participants hospitalized with COVID-19 pneumonia (the PHC group in our study), direct damage to the lungs caused by the virus and resultant inflammatory sequelae may cause longer-lasting microstructural abnormalities. Indeed, although the CT scans were normal or near normal in the PHC participants, a faint footprint of prior COVID-19 pneumonia, when present, may at least partially explain the abnormal RBC:TP and pulmonary gas transfer values. In contrast, in the NHLC participants, all the CT scans were normal, and none of the participants had evidence of previous pneumonia (accepting that this may have been because they were not imaged during their acute infection). This could indicate that the abnormalities detected in the NHLC cohort have a different pathophysiologic basis. Furthermore, DLCO , which also provides a measure of pulmonary vascular integrity, was lower in the NHLC group than in the PHC group and correlates with the RBC:TP ratio, reinforcing the significance of the findings and the need for

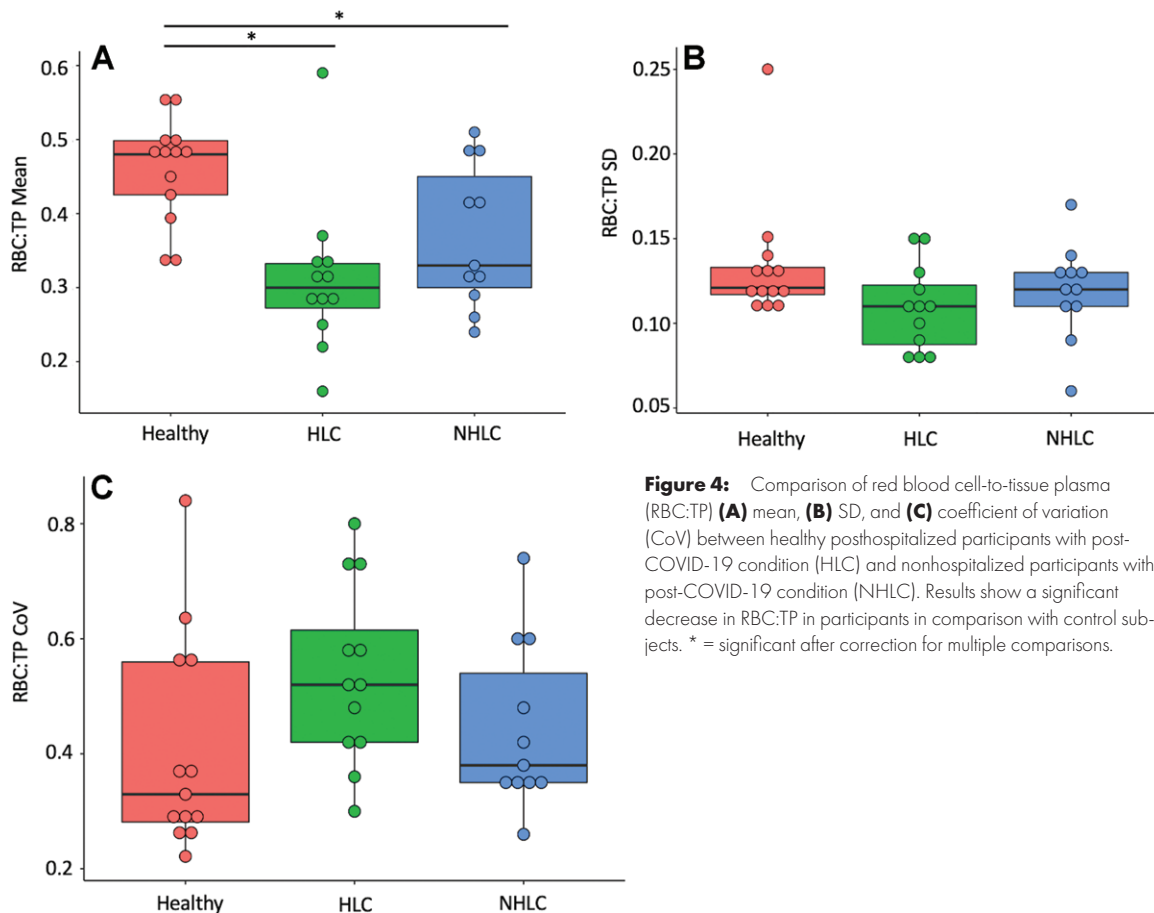


Figure 4: Comparison of red blood cell-to-tissue plasma (RBC:TP) (A) mean, (B) SD, and (C) coefficient of variation (CoV) between healthy posthospitalized participants with post-COVID-19 condition (HLC) and nonhospitalized participants with post-COVID-19 condition (NHLC). Results show a significant decrease in RBC:TP in participants in comparison with control subjects. * = significant after correction for multiple comparisons.

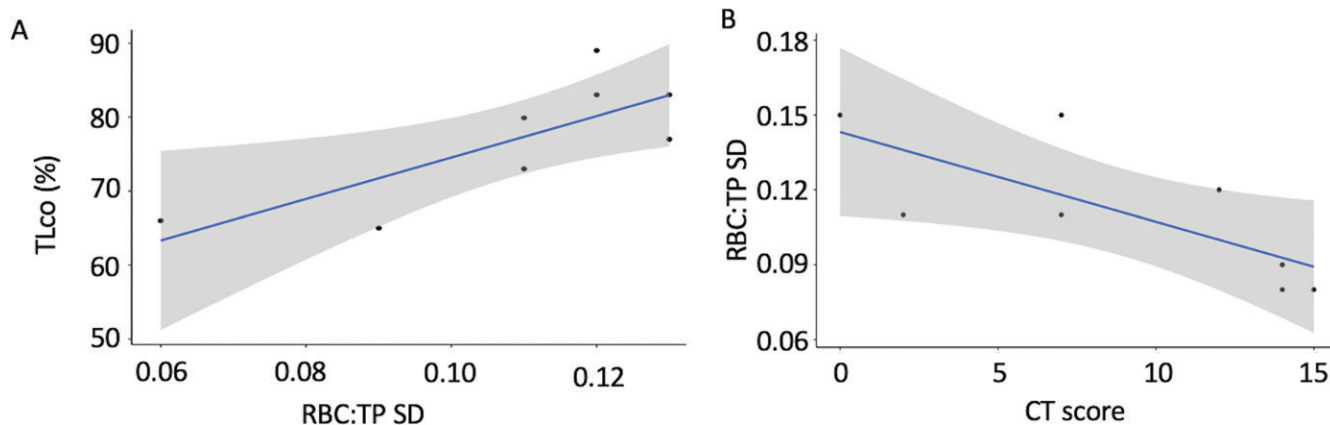


Figure 5: Correlation results. There were significant positive correlations between (A) gas transfer (D_{LCO}) and red blood cell-to-tissue plasma (RBC:TP) SD in the NHLC group and (B) RBC:TP SD and CT score in the PHC group. Results show that abnormally low D_{LCO} measurements are linked to changes in RBC:TP.

further investigation to delineate the nature of the abnormality. To further reinforce the reliability of these results, we note that previous findings have shown ^{129}Xe MRI to be a reproducible technique in both participants and volunteers and have shown a similar decreased RBC:TP, as previously seen (3). We also performed repeat imaging in a subset of PHC participants and again confirmed excellent repeatability of mean RBC:TP.

Outside of the setting of SARS-CoV-2 infection, prior studies with HP ^{129}Xe MRI in participants with interstitial lung disease diagnosed at CT have shown that more severe disease as

determined with D_{LCO} correlates with worsening RBC:TP and that HP ^{129}Xe MRI may be used to identify lung abnormalities in areas that appear normal on CT scans (17). HP ^{129}Xe MRI also appears to be more sensitive than CT in the detection of disease in participants with post-COVID-19 condition and may be a useful tool in its diagnosis, quantification, and follow-up. However, caution is necessary, as it is unknown whether participants with other respiratory tract infections, such as flu, have abnormal HP ^{129}Xe MRI gas transfer months after infection, even when they are not hospitalized and have normal CT findings. It is also not

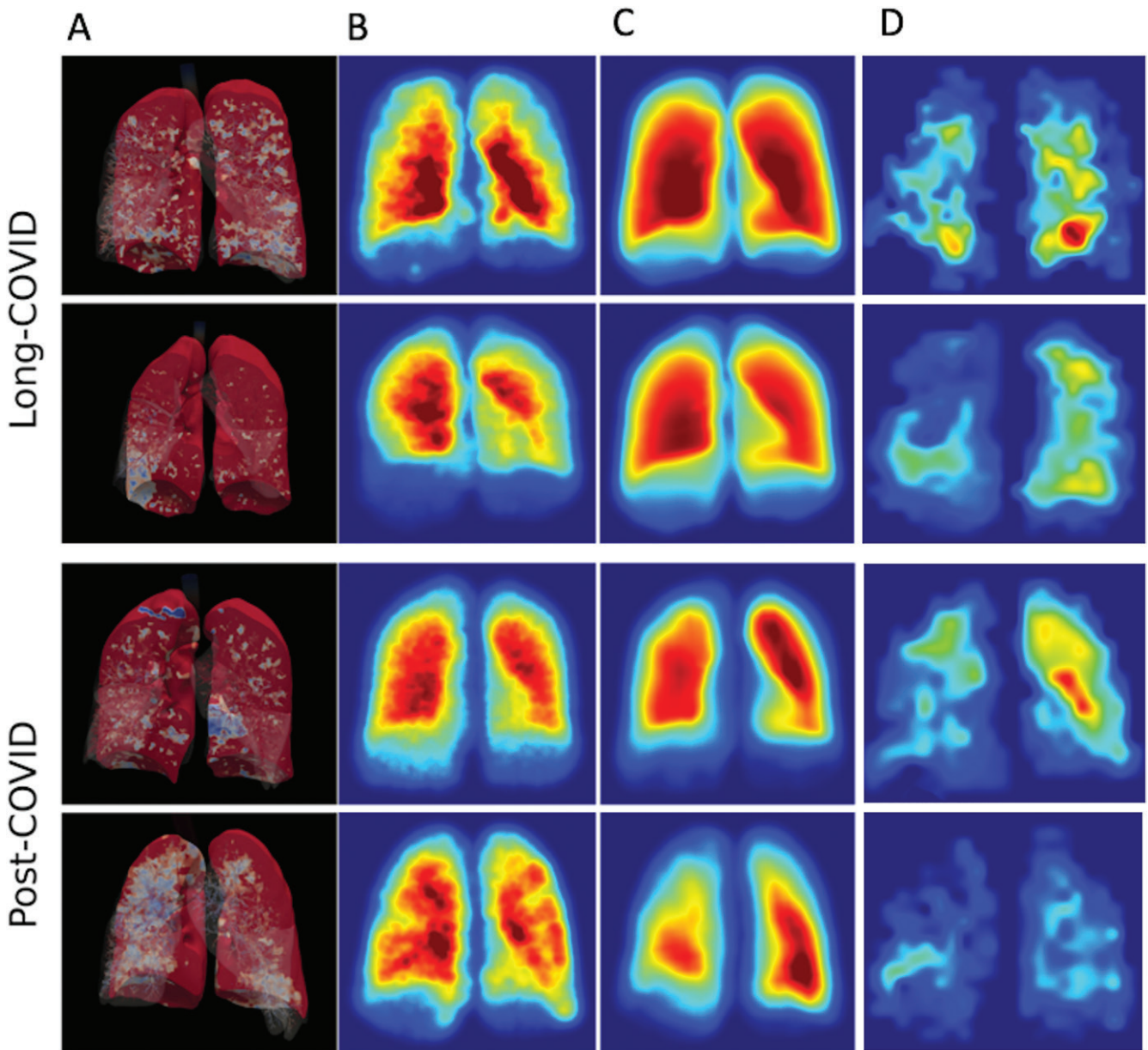


Figure 6: Three-dimensional rendering of (A) full-scale airway network (FAN), (B) FAN modeling, and (C, D) hyperpolarized xenon imaging in NHLC (C) and PHC (D) participants. Results from both low-resolution and ventilation imaging are similar and did not correlate with clinical or dissolved-phase imaging results.

known whether the abnormalities we have detected are of clinical importance, nor is it known if HP Xe MRI is an overly sensitive test, although the correlation with D_{LCO} argues against this.

The FAN model has been shown to accurately reflect regional ventilation (9). A recent study using FAN modeling in patients after COVID-19 pneumonia has confirmed that in patients with normal CT scans there are no clinically relevant detectable ventilation changes (18). The lack of significant correlation between FAN and dissolved-phase imaging findings we are reporting is in keeping with this finding, suggesting that in patients without detectable CT abnormalities, presence of continuing disease in the microvasculature and walls of the alveolar sac is the cause of ongoing breathlessness in individuals with post-COVID-19 dyspnea.

There are limitations to this study. Only small cohorts of PHC and NHLC participants were examined. Extrapolation

of these results to the worldwide population with breathlessness associated with the post-COVID-19 condition must be performed with caution. We note that a power analysis showed a need for four more participants in the NHLC cohort to begin to see significant associations between RBC:TP and quality-of-life scores. Furthermore, there is a need to repeat this study in a similar cohort at another site using power calculations (19). Older NHLC participants should be included in future studies to better assess for differences in RBC:TP with age. To better understand the significance of our findings, in the future, we plan to recruit a larger cohort of participants that includes NHLC participants without clinically relevant breathlessness alongside participants with prior proven COVID-19 infection who have fully recovered. We will also be performing repeat imaging at different intervals

of up to 12 months to determine whether the abnormalities detected persist or resolve over time.

In conclusion, hyperpolarized xenon 129 MRI has been used to identify objective impairment in gas transfer in the lungs of nonhospitalized dyspneic participants with post-COVID-19 condition and normal CT findings, providing preliminary evidence that lung abnormalities exist that cannot be detected with conventional imaging. The importance and underlying pathophysiology of this abnormality is currently unknown and highlights the need for further research in this field.

Acknowledgments: We thank Barry Johnson for his help with and support of this study. We also thank the C-MORE research team for their support of this study.

Author contributions: Guarantors of integrity of entire study, **M.D., B.R., F.G.**; study concepts/study design or data acquisition or data analysis/interpretation, all authors; manuscript drafting or manuscript revision for important intellectual content, all authors; approval of final version of submitted manuscript, all authors; agrees to ensure any questions related to the work are appropriately resolved, all authors; literature research, **J.T.G., M.C., M.D., P.A.R., J.M.W., E.F., F.G.**; clinical studies, **J.T.G., H.W., M.C., G.A.E., V.M., K.J., S.C., A.E., M.D., A.M., R.T., B.R., J.M.W., E.F., F.G.**; statistical analysis, **J.T.G., G.J.C., M.K., M.D., J.M.W., F.G.**; and manuscript editing, **J.T.G., G.J.C., M.K., A.L., V.M., K.J., M.D., A.M., R.F.S., B.R., P.A.R., J.M.W., E.F., F.G.**

Disclosures of conflicts of interest: **J.T.G.** No relevant relationships. **G.J.C.** No relevant relationships. **H.W.** No relevant relationships. **M.K.** No relevant relationships. **M.C.** No relevant relationships. **G.A.E.** No relevant relationships. **A.L.** No relevant relationships. **V.M.** No relevant relationships. **K.J.** No relevant relationships. **S.C.** No relevant relationships. **A.E.** No relevant relationships. **M.D.** No relevant relationships. **A.M.** No relevant relationships. **R.T.** British Heart Foundation intermediate clinical fellowship; institutional funding from Janssen-Cilag; support to attend meetings from Janssen-Cilag. **R.F.S.** GE Healthcare employee; stock options in GE Healthcare. **B.R.** Grants from British Heart Foundation and Oxford Centre of Research Excellence. **P.A.R.** No relevant relationships. **J.M.W.** No relevant relationships. **E.F.** Conference presentations for palliative care general medicine national training course; on the Celltrion advisory board for Regdanvimab **F.G.** Equipment from Polarean and GE Healthcare; grant from Innovate UK; consulting fees from Sensyne; on the advisory boards of AstraZeneca and Polarean; president of the European Society of Thoracic Imaging; stock in Optellum, RAIQC, and OxSonic.

References

- Huang C, Huang L, Wang Y, et al. 6-month consequences of COVID-19 in patients discharged from hospital: a cohort study. *Lancet* 2021;397(10270):220–232.
- World Health Organization. A clinical case definition of post COVID-19 condition by a Delphi consensus, 6 October 2021. https://www.who.int/publications/i/item/WHO-2019-nCoV-Post_COVID-19_condition-Clinical_case_definition-2021.1. Accessed September 12, 2021.
- Han X, Fan Y, Alwalid O, et al. Six-month Follow-up Chest CT findings after Severe COVID-19 Pneumonia. *Radiology* 2021;299(1):E177–E186.
- Pan F, Yang L, Liang B, et al. Chest CT Patterns from Diagnosis to 1 Year of Follow-up in Patients with COVID-19. *Radiology* 2022;302(3):709–719.
- Grist JT, Chen M, Collier GJ, et al. Hyperpolarized ¹²⁹Xe MRI Abnormalities in Dyspneic Participants 3 Months after COVID-19 Pneumonia: Preliminary Results. *Radiology* 2021;301(1):E353–E360.
- Qing K, Ruppert K, Jiang Y, et al. Regional mapping of gas uptake by blood and tissue in the human lung using hyperpolarized xenon-129 MRI. *J Magn Reson Imaging* 2014;39(2):346–359.
- Motiejunaite J, Balagny P, Arnoult F, et al. Hyperventilation as one of the mechanisms of persistent dyspnoea in SARS-CoV-2 survivors. *Eur Respir J* 2021;58(2):2101578.
- Collier GJ, Eaden JA, Hughes PJC, et al. Dissolved ¹²⁹Xe lung MRI with four-echo 3D radial spectroscopic imaging: Quantification of regional gas transfer in idiopathic pulmonary fibrosis. *Magn Reson Med* 2021;85(5):2622–2633.
- Kim M, Doganay O, Matin TN, Povey T, Gleeson FV. CT-based Airway Flow Model to Assess Ventilation in Chronic Obstructive Pulmonary Disease: A Pilot Study. *Radiology* 2019;293(3):666–673.
- Strassmann A, Steurer-Stey C, Lana KD, et al. Population-based reference values for the 1-min sit-to-stand test. *Int J Public Health* 2013;58(6):949–953.
- Koo TK, Li MY. A Guideline of Selecting and Reporting Intraclass Correlation Coefficients for Reliability Research. *J Chiropr Med* 2016;15(2):155–163 [Published correction appears in *J Chiropr Med* 2017;16(4):346.].
- National Institute for Health and Care Excellence. RCGP and SIGN publish guideline on managing the long-term effects of COVID-19. <https://www.nice.org.uk/news/article/nice-rcgp-and-sign-publish-guideline-on-managing-the-long-term-effects-of-covid-19>. Published December 18, 2020. Accessed September 12, 2021.
- Piiper J, Scheid P. Blood-gas equilibration in lungs. In: West JB, ed. *Pulmonary Gas Exchange*. London, England: Academic Press, 1980; 131–171.
- Stewart NJ, Leung G, Norquay G, et al. Experimental validation of the hyperpolarized ¹²⁹Xe chemical shift saturation recovery technique in healthy volunteers and subjects with interstitial lung disease. *Magn Reson Med* 2015;74(1):196–207.
- Pretorius E, Vlok M, Venter C, et al. Persistent clotting protein pathology in Long COVID/Post-Acute Sequelae of COVID-19 (PASC) is accompanied by increased levels of antiplasmin. *Cardiovasc Diabetol* 2021;20(1):172.
- Roughton FJ, Forster RE. Relative importance of diffusion and chemical reaction rates in determining rate of exchange of gases in the human lung, with special reference to true diffusing capacity of pulmonary membrane and volume of blood in the lung capillaries. *J Appl Physiol* 1957;11(2):290–302.
- Mammarappallil JG, Rankine L, Wild JM, Driehuis B. New Developments in Imaging Idiopathic Pulmonary Fibrosis With Hyperpolarized Xenon Magnetic Resonance Imaging. *J Thorac Imaging* 2019;34(2):136–150.
- Inui S, Yoon SH, Doganay O, Gleeson FV, Kim M. Impaired pulmonary ventilation beyond pneumonia in COVID-19: A preliminary observation. *PLoS One* 2022;17(1):e0263158.
- Eng J. Sample size estimation: how many individuals should be studied? *Radiology* 2003;227(2):309–313.